Inorg. Chem. **2009**, *48*, 1030−1037

Blue Phosphorescent Ir(III) Complex with High Color Purity: *fac*-Tris(2′,6′-difluoro-2,3′-bipyridinato-*N,C*$^{4'}$)iridium(III)

Seok Jong Lee,[†] Ki-Min Park,[‡] Kiyull Yang,[‡] and Youngjin Kang*[,§]

LG Display Co., Ltd. 642-3, Jinpyung-dong, Gumi Gyungbuk, 730-726, Republic of Korea, Research Institute of Natural Science & Department of Chemistry Education, Gyeongsang National University, Jinju 660-701, Republic of Korea, and Division of Science Education, Kangwon National University, Chuncheon 200-701, Republic of Korea

Received August 28, 2008

A blue phosphorescent iridium(III) complex (**1**) bearing fluorine-substituted bipyridine (dfpypy) has been synthesized and characterized to investigate the effect of the substitution and replacement of the phenyl ring in ppy (phenylpyridine) with pyridine on the solid state structure and its photoluminescence. The optical properties and electrochemical behaviors of **1** have also been systematically evaluated. The structure of **1** has also been determined by a single-crystal X-ray diffraction analysis. There are varied intermolecular interactions caused by the pyridine and fluorine substituents, such as C−H···N, C−H···F, and $\pi\cdots\pi$ interactions of either face-to-face type or edge-to-face C−H···π and halogen···π in crystal packing. In electrochemistry, the remarkably higher oxidation potential than that of FIrpic was observed. The emission λ_{max} of **1** at room temperature is at 438 nm with a higher PL quantum efficiency. Complex **1** exhibits intense blue emission with high color purity (CIE $x = 0.14$, $y = 0.12$), which has been attributed to metal-to-ligand charge-transfer triplet emission based on DFT calculations.

Introduction

Luminescent complexes containing third-row transition metals have attracted much attention owing to their varied applications, such as photonics and electronics.[1] In particular, cyclometallated iridium(III) complexes are regarded as excellent phosphorescent materials and have been widely studied because of their ability to achieve maximum internal quantum efficiency, nearly 100%, as well as high external quantum efficiency in OLEDs.[2] Cyclometallated $(C\wedge N)_3Ir(III)$ complexes with facial geometry have shown high thermal stability and high phosphorescent efficiency, and hence their derivatives are promising phosphorescent metal complexes in OLEDs.[3] Luminescent $Ir(ppy)_3$ (ppy = 2-phenylpyridine) derivatives have been widely investigated because the emission wavelength of $Ir(ppy)_3$ can be readily controlled either by the introduction of electron-donating and/or electron-withdrawing groups into the ppy ligand or by derivatization of the C∧N chelating modes using benzothiophene and quinoline.[4] For example, Thompson and Forrest et al. reported blue and red emission energies by the introduction of a fluorine group into the phenyl ring for the

* To whom correspondence should be addressed. Phone: +82-33-250-6737. Fax: +82-33-242-9598. E-mail: kangy@kangwon.ac.kr.
† LG Display Co., Ltd 642-3.
‡ Gyeongsang National University.
§ Kangwon National University.

(1) (a) Walzer, K.; Maennig, B.; Pfeiffer, M.; Leo, K. *Chem. Rev.* **2007**, *107*, 1233–1271, and references cited therein. (b) Segal, M.; Singh, M.; Rivoire, K.; Difley, S.; Voorhis, T. V.; Baldo, M. A. *Nature* **2007**, *6*, 374–378. (c) Chou, P.-T.; Chi, Y. *Chem. Eur. J.* **2007**, *13*, 380–395. (d) Kalyanasundaram, K.; Grätzel, M. *Coord. Chem. Rev.* **1998**, *177*, 347–414.

(2) (a) Baldo, M. A.; Thompson, M. E.; Forrest, S. R. *Nature* **2000**, *403*, 750–753. (b) Baldo, M. A.; Lamansky, S.; Burrows, P. E.; Thompson, M. E.; Forrest, S. R. *Appl. Phys. Lett.* **1999**, *75*, 4–6. (c) Adachi, C.; Baldo, M. A.; Forrest, S. R.; Thompson, M. E. *Appl. Phys. Lett.* **2000**, *77*, 904–906. (d) Yuichiro Kawamura, Y.; Goushi, K.; Brooks, J.; Brown, J. J.; Sasabe, H.; Adachi, C. *Appl. Phys. Lett.* **2005**, *86*, 071104. (e) Adachi, C.; Baldo, M. A.; Forrest, S. R. *J. Appl. Phys.* **2001**, *90*, 5048–5051.

(3) (a) Tamayo, A. B.; Alleyne, B. D.; Djurovich, P. I.; Lamansky, S.; Tsyba, I.; Ho, N. N.; Bau, R.; Thompson, M. E. *J. Am. Chem. Soc.* **2003**, *125*, 7377–7387. (b) Ostrowski, J. C.; Robinson, M. R.; Heeger, A. J.; Bazan, G. C. *Chem.Commun.* **2002**, 784–785. (c) Adamovich, V.; Brooks, J.; Tamayo, A.; Djurovich, P.; Alexander, A.; Thompson, M. E. *New J. Chem.* **2002**, 1171–1178. (d) Xie, H. Z.; Liu, M. W.; Wang, O. Y.; Zhang, X. H.; Lee, C. S.; Hung, L. S.; Lee, S. T.; Teng, P. F.; Kwong, H. L.; Zheng, H.; Che, C. M. *Adv. Mater.* **2001**, *13*, 1245–1248. (e) Kang, D. M.; Kang, J.-W.; Park, J. W.; Jung, S. O.; Lee, S.-H.; Park, H.-D.; Kim, Y.-H.; Shin, S. C.; Kim, J.-J.; Kwon, S.-K. *Adv. Mater.* **2008**, *20*, 2003–2007.

(4) (a) Grushin, V. V.; Herron, N.; LeCloux, D. D.; Marshall, W. J.; Petrov, V. A.; Wang, Y. *Chem. Commun.* **2001**, 1494–1495. (b) Sajoto, T.; Djurovich, P. I.; Tamayo, A.; Yousufuddin, M.; Bau, R.; Thompson, M. E.; Holmes, R. J.; Forrest, S. R. *Inorg. Chem.* **2005**, *44*, 7992–8003.

10.1021/ic801643p CCC: $40.75
Published on Web 12/22/2008

former, and by using a quinoline unit instead of a pyridine ring for the latter. In addition, the emission energy can be fine-tuned by the combination of auxiliary (two *o*-chelating (C∧N) ligands) and LX type of ancillary ligands (*e.g.*, monoanionic chelating ligands, *acac* = acetylacetone, *pic* = picolinate, *sal* = salicylimine, *iq* = isoquinolinecarboxylate, *bpz* = pyrazolylborate).[5]

To achieve full color display, three primary colors, such as blue, green, and red, are necessary. However, homoleptic Ir(III) complexes with both blue emission at room temperature and facial geometry are very rare, compared to those of phosphorescent green and red.[4b,6] The following considerations should be needed for the development of blue phosphorescent Ir(III) complexes: (i) the adoption of a ligand with large triplet energy, since the emission energies of cyclometallated Ir(III) complexes are mainly determined by the triplet energy of the C∧N chelating ligand, and (ii) the inducement of a larger band gap by stabilizing the HOMO and destabilizing the LUMO level.

Recently, the Tamao group reported that pyridine has lower HOMO and LUMO energy levels than those of some nitrogen-containing heterocyclic compounds. Moreover, the pyridine ring is more electronegative than a nonsubstituted phenyl ring.[7] These facts prompted us to develop a new C∧N chelating bipyridine (bpy or pypy) ligand, as opposed to the phenylpyridine (ppy) ligand system.

Herein, we describe the results of our investigation on the preparation, structural characterization, electrochemical behavior, and photophysical properties of the *fac*-Ir(dfpypy)$_3$ (dfpypy = 2′,4′-difluoro-2,3′-bipyridinato-*N*,$C^{4'}$) complex.

Experimental Section

General Considerations. All experiments were performed under a dry N_2 atmosphere using standard Schlenk techniques. All solvents were freshly distilled over appropriate drying reagents prior to use. All starting materials were purchased from either Aldrich or Strem and used without further purification.

Measurement. ^{1}H NMR and mass spectra were recorded on a Bruker DRX 400 MHz spectrometer and JEOL-JMS 700 instrument, respectively. UV/vis and photoluminescent spectra for all samples with concentrations in the range of 10−50 μM were obtained from the UV/vis spectrometer Lambda 900 and a Perkin-Elmer luminescence spectrometer LS 50B, respectively. All solutions for photophysical experiments were degassed with more than three repeated freeze−pump−thaw cycles in a vacuum line. Cyclic voltammetry was performed with an Autolab potentiostat by Echochemie under a nitrogen atmosphere in a one-compartment electrolysis cell consisting of a platinum wire working electrode, a platinum wire counter electrode, and a quasi Ag/AgCl reference electrode. Cyclic voltammograms were monitored at scan rates of either 100 or 50 mV s^{-1} and recorded in distilled dichloromethane/acetonitrile. The concentration of the complex was maintained at 0.5 mM or less, and each solution contained 0.1 M tetrabutylammonium hexafluorophosphate (TBAP) as the electrolyte. The thermogravimetric spectrum was recorded on a Perkin-Elmer TGA-7 under nitrogen environment at a heating rate of 10 °C/min over a range of 25−700 °C.

Theoretical Calculations. Computations on the electronic ground state of **1** were performed using Becke's three-parameter density functional in combination with the nonlocal correlation functional of Lee, Yang, and Parr (B3LYP).[8] 6-31G(d) basis sets were employed for the ligand and the relativistic effective core potential of Los Alamos and double-ζ basis sets were employed for the Ir (LANL2DZ).[9] The ground-state geometries were fully optimized at the B3LYP level, and time-dependent DFT (TDDFT)[10a] calculations were preformed to obtain the vertical singlet and triplet excitation energies. All computations were performed using the Gaussian-98 package.[10b]

X-ray Crystallographic Analysis. Suitable crystals of **1** were obtained from slow vapor diffusion of hexane into a solution of **1** in dichloromethane/benzene. The single crystal of **1** was attached to glass fibers and mounted on a Bruker SMART diffractometer equipped with graphite monochromated Mo Kα (λ = 0.710 73 Å) radiation, operating at 50 kV and 30 mA with a CCD detector; 45 frames of two-dimensional diffraction images were collected and processed to obtain the cell parameters and orientation matrix. All data collections were performed at 173(2) K. The data collection 2θ range was 3.7−53.0°. No significant decay was observed during the data collection. The raw data were processed to give structure factors using the SAINT-plus program.[11a] Empirical absorption corrections were applied to the data sets using the SADABS.[11b] The structure was solved by direction methods and refined by full-matrix least-squares against F^2 for all data using SHELXTL software.[11c] All non-hydrogen atoms in compound **1** were anisotropically refined. All hydrogen atoms were included in the calculated positions and refined using a riding model with isotropic thermal parameters 1.2 times those of the parent atoms. The compound **1** cocrystallizes with benzene/0.7 dichloromethane, and

(5) (a) You, Y.; Park, S. Y. *J. Am. Chem. Soc.* **2005**, *127*, 12438–12439. (b) Li, J.; Djurovich, P. I.; Alleyne, B. D.; Tsyba, I.; Ho, N. N.; Bau, R.; Thompson, M. E. *Polyhedron* **2004**, *23*, 419–428. (c) Lamansky, S.; Djurovich, P.; Murphy, D.; Abdel-Razzaq, F.; Kwong, R.; Tsyba, I.; Bortz, M.; Mui, B.; Bau, R.; Thompson, M. E. *Inorg. Chem.* **2001**, *40*, 1704–1711. (d) Lamansky, S.; Djurovich, P.; Murphy, D.; Abdel-Razzaq, F.; Lee, H.-E.; Adachi, C.; Burrows, P. E.; Forrest, S. R.; Thompson, M. E. *J. Am. Chem. Soc.* **2001**, *123*, 4304–4312. (e) Kwon, T.-H.; Cho, H. S.; Kim, M. K.; Kim, J.-W.; Kim, J.-J.; Lee, K. H.; Park, S. J.; Shin, I.-S.; Kim, H.; Shin, D. M.; Chung, Y. K.; Hong, J.-I. *Organometallics* **2005**, *24*, 1578–1585.

(6) (a) Yeh, Y.-S.; Cheng, Y.-M.; Chou, P.-T.; Lee, G.-H.; Yang, C.-H.; Chi, Y.; Shu, C.-F.; Wang, C.-H. *Chem. Phys. Chem.* **2006**, *7*, 2294–2297, and references cited therein. (b) Chew, S.; Lee, C. S.; Lee, S.-T.; Wang, P.; He, J.; Li, W.; Pan, J.; Zhang, X.; Kwong, H. *Appl. Phys. Lett.* **2006**, *88*, 93510.

(7) Tamao, K.; Uchida, M.; Izumizawa, T.; Furukawa, K.; Yamaguchi, S. *J. Am. Chem. Soc.* **1996**, *118*, 11974–11975.

(8) (a) Becke, A. D. *J. Chem. Phys.* **1993**, *98*, 5648–5652. (b) Lee, C.; Yang, W.; Parr, R. G. *Phys. Rev. B* **1988**, *37*, 785–789.

(9) Hay, P. J. *J. Phys. Chem. A* **2002**, *106*, 1634–1641.

(10) (a) Jarmorski, C.; Casida, M. E.; Salahub, D. R. *J. Chem. Phys.* **1996**, *104*, 5134–5147. (b) Frisch, M. J.; Trucks, G. W.; Schlegel, H. B.; Scuseria, G. E.; Robb, M. A.; Cheeseman, J. R.; Zakrzewski, V. G.; Montgomery, J. A., Jr.; Stratmann, R. E.; Burant, J. C.; Dapprich, S.; Millam, J. M.; Daniels, A. D.; Kudin, K. N.; Strain, M. C.; Farkas, O.; Tomasi, J.; Barone, V.; Cossi, M.; Cammi, R.; Mennucci, B.; Pomelli, C.; Adame, C.; Clifford, S.; Ochterski, J.; Petersson, G. A.; Ayala, P. Y.; Cui, Q.; Morokuma, K.; Salvador, P.; Dannenberg, J. J.; Malick, D. K.; Rabuck, A. D.; Raghavachari, K.; Foresman, J. B.; Cioslowski, J.; Ortiz, J. V.; Baboul, A. G.; Stefanov, B. B.; Liu, G.; Liashenko, A.; Piskorz, P.; Komaromi, I.; Gomperts, R.; Martin, R. L.; Fox, D. J.; Keith, T.; Al-Laham, M. A.; Peng, C. Y.; Nanayakkara, A.; Challacombe, M.; Gill, P. M. W.; Johnson, B.; Chen, W.; Wong, M. W.; Andres, J. L.; Gonzalez, C.; Head-Gordon, M.; Replogle, E. S.; Pople, J. A. Gaussian 98, Revision A.7; Gaussian, Inc.: Pittsburgh, PA, 1998.

(11) (a) Bruker, SMART (ver. 5.625) and SAINT-plus (ver. 6.22). *Area Detector Control and Integration Software*; Bruker AXS Inc.: Madison, WI, 2000. (b) Bruker, SADABS (ver. 2.03). *Empirical absorption and correction software*; Bruker AXS Inc.: Madison, WI, 1999. (c) Bruker, SHELXTL (ver. 6.10). *Program for Solution and Refinement of Crystal Structures*; Bruker AXS Inc.: Madison, WI, 2000.

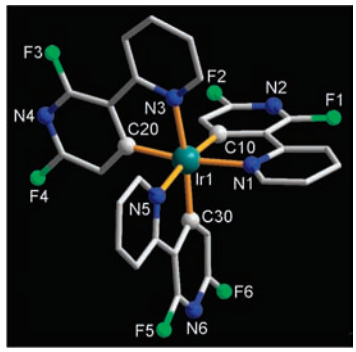

Figure 1. Coordination environment of the Ir(III) ion in complex **1** with selected numbering scheme. Selected bond lengths (Å) and angles (deg): Ir1−C10 2.001(5), Ir1−C20 1.997(5), Ir1−C30 2.005(5), Ir1−N1 2.115(4), Ir1−N3 2.136(4), Ir1−N5 2.1278(4), C10−Ir1−C20 93.9(2), C10−Ir1−C30 92.9(2), C10−Ir1−N1 79.7(2), C10−Ir1−N3 93.72(18), C10−Ir1−N5 171.57(19), C20−Ir1−C30 97.0(2), C20−Ir1−N1 171.26(19), C20−Ir1−N3 79.5(2), C20−Ir1−N5 90.74(19), C30−Ir1−N1 89.24(19), C30−Ir1−N3 172.72(19), C30−Ir1−N5 79.52(19), N1−Ir1−N3 94.93(17), N1−Ir1−N5 96.40(17), N5−Ir1−N3 94.06(16).

Table 1. Crystal Data and Structure Refinement for **1**

empirical formula	$[IrC_{30}H_{15}N_6F_6](C_6H_6)(CH_2Cl_2)_{0.7}$
formula weight	903.24
crystal system	monoclinic
space group	$P2_1/n$
a (Å)	15.3684(8)
b (Å)	10.3143(5)
c (Å)	22.4069(12)
β (deg)	104.8030(10)
V (Å^3)	3433.9(3)
Z	4
D(calcd) (g cm^{-3})	1.747
μ (mm^{-1})	4.067
F(000)	1758
scan type	φ-ω
no. of reflections collected	19 755
no. of independent reflections	7077 (R_{int} = 0.0267)
absorption correction	empirical (SADABS)
goodness of fit	1.092
R_1, wR_2 [$I > 2\sigma(I)$]	0.0393, 0.1008
R_1, wR_2 (all data)	0.0460, 0.1041

the crystal system is the monoclinic space group $P2_1/n$. The solvent molecules were modeled successfully. Crystal data for **1** is summarized in Table 1. Selected bond lengths and angles for **1** are given in Figure 1. The refined atomic coordinates and anisotropic thermal parameters are deposited in the Supporting Information. Crystallographic data (cif files for **1**) for the structure reported here have been deposited with the Cambridge Crystallographic Data Center (Deposition No. CCDC-698914). The data can be obtained free of charge via http://www.ccdc.cam.ac.uk. /perl/catreq/catreq.cgi (or from the CCDC, 12 Union Road, Cambridge CB2 1EZ, UK; fax, +44 1223 336033; e-mail, deposit@ccdc.cam.ac.uk).

Syntheses. 2,6-Difluoropyridyl-3-boronic Acid. A stirred solution of diisopropylamine (1.7 mL, 12 mmol) in diethyl ether (20 mL) was cooled to −78 °C. Addition of *n*-BuLi (22.5 mL, 36 mmol, 1.6 M in hexane) over 20 min resulted in a pale yellow solution. After stirring for 1 h at this temperature, 2,6-difluoropyridine (0.91 mL, 10 mmol) was added. The solution was stirred for an additional hour, and then trimethyl borate (1.4 mL, 12.5 mmol) was added at −78 °C. The mixture was allowed to warm to room temperature and to react for 1 h. The mixture was quenched by the slow addition of 5% aqueous NaOH solution (20 mL). After 10 min, the mixture was acidified by the dropwise addition of 3 N HCl. Extraction with ethyl acetate and evaporation of the organic layer furnished the pure title compound, which was obtained as a white solid in 90% yield. ^{1}H NMR ($CDCl_3$): δ 8.4 (q, J = 8 Hz, 1H), 6.9 (m, 1H), 5.3 (s, 2H). Anal. Calcd for $C_5H_4BF_2NO_2$: C, 37.79; H, 2.54; N, 8.81. Found: C, 37.75; H, 2.58; N, 8.79.

Ligand dfpypy (L_1). 2-Bromopyridine (0.31 mL, 3.99 mmol), 2,6-difluoropyridyl-3-boronic acid (0.76 g, 4.78 mmol), and Pd(PPh_3)$_4$ (0.28 g, 0.24 mmol) were dissolved in THF (25 mL). A solution of 5% K_2CO_3 (10 mL) was added, and the mixture was refluxed with stirring for 18 h under a nitrogen atmosphere. After being cooled, the mixture was poured into water and extracted with ethyl acetate. The organic layer was dried over $MgSO_4$. The solvent was removed under reduced pressure to give a crude residue. The crude product was purified by column chromatography on silica gel (EtOAc/hexane, 1/3, v/v) to obtain a colorless solid (65%). ^{1}H NMR ($CDCl_3$): δ 8.57 (m, 2H), 7.69 (m, 2H), 7.18 (m, 1H), 6.87 (m, 1H). Anal. Calcd for $C_{10}H_6F_2N_2$: C, 62.50; H, 3.15; N, 14.58. Found: C, 62.48; H, 3.14; N, 14.60.

Complex Ir(dfpypy)$_3$ (1). Ligand dfpypy (1.92 g, 10.0 mmol) and Ir(acac)$_3$ (1.22 g, 2.50 mmol) were dissolved in ethylene glycol (50 mL), and the mixture was heated to reflux under nitrogen for 25 h. The reaction mixture was then cooled to room temperature, 1 N HCl was added, and the mixture was filtered to give a crude product, which was flash chromatographed on a silica column using dichloromethane to yield 0.31 g (20%) of material. The compound was then further purified by sublimation. ^{1}H NMR (CD_2Cl_2): δ 8.36 (d, J = 8 Hz, 3H), 7.89 (dt, J = 8 Hz, 2 Hz, 3H), 7.52 (dd, J = 5 Hz, 1 Hz, 3H), 7.13 (m, 3H), 6.25 (t, J = 2 Hz, 3H). ^{13}C NMR (CD_2Cl_2): δ 180.7, 162.8, 160.8, 147.8, 139.0, 124.3, 124.1, 123.9, 113.0, 112.7 (C−F resonance not located). MS (FAB): m/z = 767 [M$^+$]. Anal. Calcd for $C_{30}H_{15}F_6N_6Ir$: C, 47.06; H, 1.97; N, 10.98. Found: C, 47.10; H, 1.95; N, 10.95.

Result and Discussion

The fluorinated bipyridine ligand was synthesized using a Suzuki coupling by the reaction of 2-bromopyridine with 2,6-difluoropyridinyl-3-boronic acid in the presence of K_2CO_3 and Pd(PPh_3)$_4$ as a catalyst, as shown in Scheme 1. This ligand was obtained in good yields (∼85%). Complex **1** was synthesized by a slight modification of a previous synthetic methodology reported by Watt et al.[12] By the reaction of Ir(acac)$_3$ with the ligand at high temperature (>200 °C), complex **1** was obtained in a moderate yield (*ca.* 20∼40%).

Complex **1** is very stable under air and was fully characterized by NMR, mass spectrometry, and elemental analysis (see Supporting Information). In the ^{1}H NMR spectrum, the complex exhibits five well-resolved peaks in the region of 6.0∼8.5 ppm due to the pyridine rings, indicating that the complex has facial geometry around the Ir atom. Two peaks at −69 and −73 ppm in the ^{19}F-NMR spectrum were observed as doublets due to the coupling of the neighboring F atom. The coupling constant ($^4J_{F-F}$) was 9.87 Hz, which is agreement with a previous report.[13] To investigate the thermal stability of **1**, thermogravimetric analysis (TGA) was conducted. No loss of weight was observed in the range below 250 °C, and the decomposition temperature, which is defined as a 5% loss of weight,

(12) (a) Dedeian, K.; Djurovich, P. I.; Garces, F. O.; Carlson, G.; Watt, R. J. *Inorg. Chem.* **1991**, *30*, 1687–1688. (b) Jung, S.; Kang, Y.; Kim, H.-S.; Kim, Y.-H.; Lee, C.-L; Kim, J.-J; Lee, S.-K; Kwon, S.-K. *Eur. J. Inorg. Chem.* **2004**, *17*, 3415–3423.

(13) Dedeian, K.; Shi, J.; Shepherd, N.; Forsythe, E.; Morton, D. C. *Inorg. Chem.* **2005**, *44*, 4445–4447.

Scheme 1. Synthetic Routes and Structures of $\mathbf{L_1}$ and **1** Used in This Study

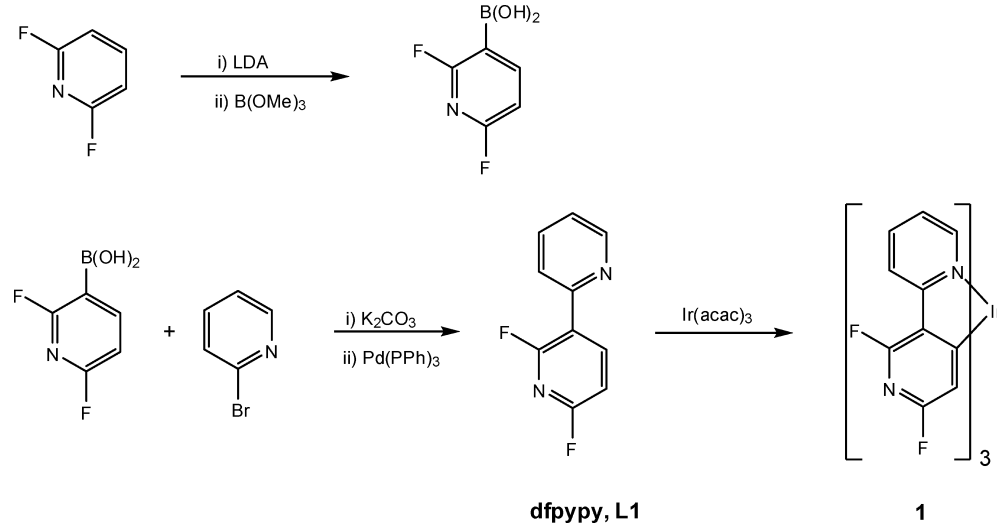

appeared at 452 °C. This result indicates that complex **1** has high thermal stability and is much more stable than *fac*-[Ir(ppy)$_3$](423 °C).[14] The observed high thermal stability seems to be caused by the F atom introduced onto the pyridine backbone, in that, by the general rule of thumb, the F atom induces sublimity of a compound and increases the thermal stability by strong C−F bond.

The structure of **1** was unambiguously established by single-crystal X-ray diffraction analysis. The crystal structure and packing diagram of **1** are presented in Figure 1 and Figure 2, respectively. Complex **1** in the crystal structure exhibits only facial configuration with distorted octahedral geometry around the Ir atom, as shown in Figure 1.

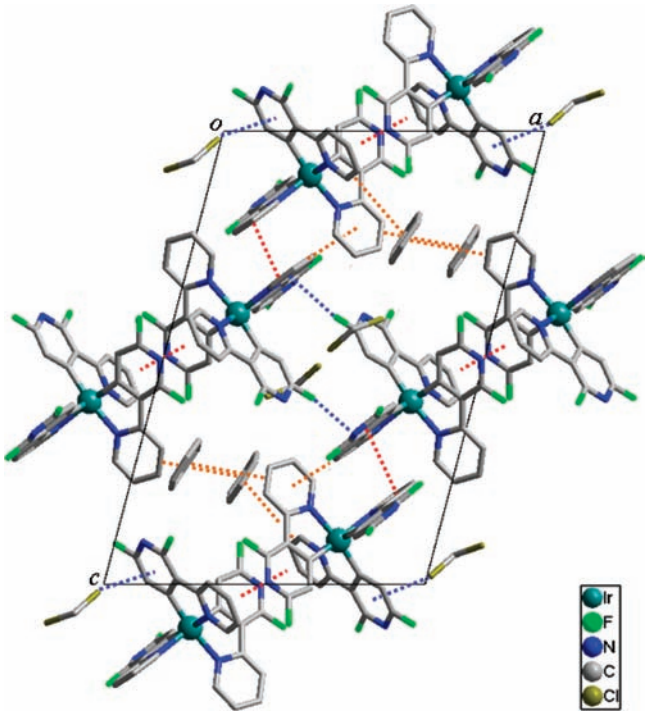

Figure 2. Crystal packing structure of **1**. Dotted lines represent intermolecular interactions: face-to-face $\pi\cdots\pi$, brown; halogen$\cdots\pi$, blue. The C−H$\cdots$X (X = N or F) hydrogen bonds are not shown for clarity.

The range of dihedral angles between two pyridine rings of each ligand in **1** is 3.8(4)−5.6(3)°, indicating that the two pyridine rings are almost coplanar. The Ir−C bond length, ranging from 1.997(5) to 2.005(5) Å, is slightly shorter than those of other mononuclear complexes with blue emission (Ir−C = 2.015(7)∼2.027(6) Å for *fac*-Ir(ppz)$_3$; Ir−C = 2.019(7)∼2.024(8) Å for *fac*-Ir(flz)$_3$).[4b] Furthermore, the C−C and C−N bond lengths and angles are within normal ranges and are in agreement with corresponding parameters described for other similarly constituted complexes.[15] All σ-donor C atoms (C10, C20, and C30) in metallated difluoronated pyridine ligands arrange a *trans* placement to dative N atoms (N5, N6, and N3) in the adjacent pyridine ring. The Ir−N bond lengths (2.116(4)∼2.135(4) Å) observed in **1** are in agreement with those of *fac*-Ir(flz)$_3$ (flz = 1-[9,9,-dimethyl-2fluorenyl])pyrazolyl) (2.095(7)∼2.121(6) Å), and *fac*-Ir(ppz)$_3$ (1-phenylpyrazoly-*N*,$C^{2\prime}$) (2.117(5)∼2.135(5) Å).[4b] The crystal packing of **1**, as shown in Figure 2, is mainly stabilized by two kinds of the intermolecular interactions. One is weak hydrogen bonding such as the C−H$\cdots$N and C−H$\cdots$F type. The distances of H$\cdots$N and H$\cdots$F are in the region of 2.41−2.67 Å (Table 2). The other is $\pi\cdots\pi$ interactions, such as the face-to-face type, with the average distance between pridyl ring planes being 3.45 Å. In addition, weak intermolecular interactions, such as edge-to-face C−H$\cdots\pi$(py)[16] and halogen$\cdots\pi$(py) interactions,[17] are also observed in the crystal packing structure. The structural parameters for the intermolecular interactions are summarized

(14) Wong, W.-Y.; Ho, C.-L; Gao, Z.-X.; Mi, B.-X.; Chen, C.-H.; Cheah, K.-W.; Lin, A. *Angew. Chem., Int. Ed.* **2006**, *45*, 7800–7803.
(15) Böttcher, H.-C.; Graf, M.; Krüger, H.; Wagner, C. *Inorg. Chem. Commun.* **2005**, *5*, 278–280.
(16) (a) Hunter, C. A.; Lawson, K. R.; Perkins, J.; Urch, C. J. *J. Chem. Soc., Perkin Trans. 2* **2001**, 651–669. (b) Jorgensen, W. L.; Severance, D. L. J. *J. Am. Chem. Soc.* **1990**, *112*, 4768–4774.
(17) (a) Schollmeyer, D.; Shishkin, O. V.; Rühl, T.; Vysotsky, M. O. *Cryst. Eng. Commun.* **2008**, *10*, 715–723. (b) Swierczynski, D.; Luboradzki, R.; Dolgonos, G.; Lipkowski, J; Schneider, H.-J. *Eur. J. Org. Chem.* **2005**, *6*, 1172–1177. (c) Desiraju, G. R.; Steiner, T. *The Weak Hydrogen Bond in Structural Chemistry and Biology*; Oxford University Press: Oxford, 1999. (d) Jetti, R. K. R.; Nangia, A.; Xue, F.; Mak, T. C. W. *Chem. Commun.* **2001**, 919–920.

Table 2. Structural Parameters of Hydrogen Bonds and Intermolecular Interactions for **1** (Å and deg)[a]

D−H···A	*d*(D−H)	*d*(H···A)	*d*(D···A)	∠(DHA)
C1−H1···F5[b]	0.95	2.46	3.096(6)	124.8
C1−H1···N6[b]	0.95	2.56	3.337(8)	138.9
C2−H2···F3[c]	0.95	2.67	3.322(7)	126.6
C13−H13···N2[d]	0.95	2.67	3.598(8)	166.2
C21−H21···F6[d]	0.95	2.41	3.087(7)	127.9
C36−H36···N4[e]	0.95	2.67	3.419(13)	135.9
C37−H37A···F3[f]	0.99	2.54	3.142(14)	119.3
$\pi\cdots\pi$ interactions				
A···A[e]			3.34(1)	0.0(3)
B[g]···C			3.55(1)	35.1(4)
C−H···π interactions				
C23−H23···Cg1[b]	0.95	2.90	3.73	145.8
halogen···π interactions				
Cl2···Cg2			3.40	
F4···Cg3[h]			2.99	

[a] A, B, and C define each pyridyl ring plane including N2, N5, and N6, respectively. Cg1 and Cg2 define the centroids of each pyridyl ring including N1 and N4, respectively. Cg3 defines the centroid of C26 and C27. Symmetry codes given in footnotes *b*−*h*. [b] $-x+0.5, y+0.5, -z+0.5$. [c] $x+0.5, -y+1.5, z+0.5$. [d] $x, y+1, z$. [e] $-x+1, -y+1, -z$. [f] $-x, -y+2, -z$. [g] $-x+0.5, y-0.5, -z+0.5$. [h] $-x, 1-y, -z$.

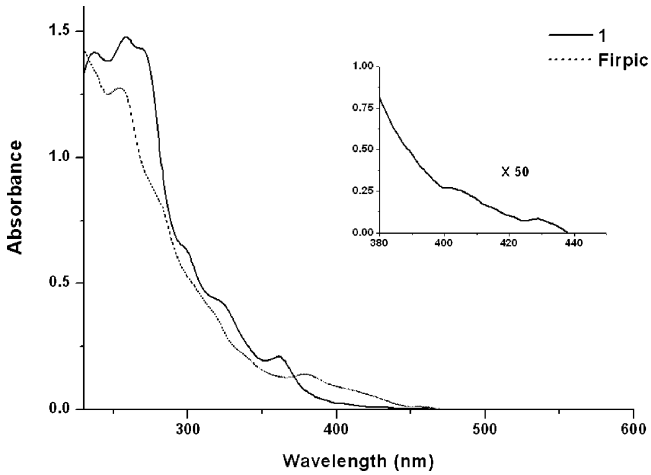

Figure 3. UV/vis absorption spectra of **1** and FIrpic at room temperature under the same conditions (concentration, 2.5×10^{-5} M; solvent, CH_2Cl_2). Inset: MLCT band of **1** in UV/vis.

in Table 2. The thermal stability of **1** may originate from these intermolecular interactions.

To examine the photophysical properties of complex **1** synthesized by using ligand $\mathbf{L_1}$, UV/vis and photoluminescent spectra were measured in a dilute CH_2Cl_2 solution. As expected, when being irradiated by UV light, complex **1** showed a bright blue emission. Therefore, the absorption and emission spectra of **1** were compared with those of FIrpic (bis(4,6-difluorophenylpyridinato-*N,C*^{2})picolinatoiridium(III)) as a reference, which has well-known blue phosphorescence.[18] Figure 3 shows the UV−visible absorption spectrum for **1** in CH_2Cl_2 at room temperature. The strong absorption band observed at 230−300 nm closely resembles the spectrum of the free ligand (see Supporting Information), which is assigned to a ligand-centered $^1\pi-\pi^*$ transition. The broad absorption bands at lower energy

(18) The CIE coordinates *x* and *y* was measured to be 0.18 and 0.22, based on our preliminary investigation on OLEDs performance using **1** as emitting material. (a) Adachi, C.; Kwong, R. C.; Djurovich, P.; Adamovich, V.; Baldo, M. A.; Thompson, M. E.; Forrest, S. R. *Appl. Phys. Lett.* **2001**, *79*, 2082. (b) Mulder, C. L.; Celebi, K.; Milaninia, K. M.; Baldo, M. A. *Appl. Phys. Lett.* **2007**, *90*, 211109.

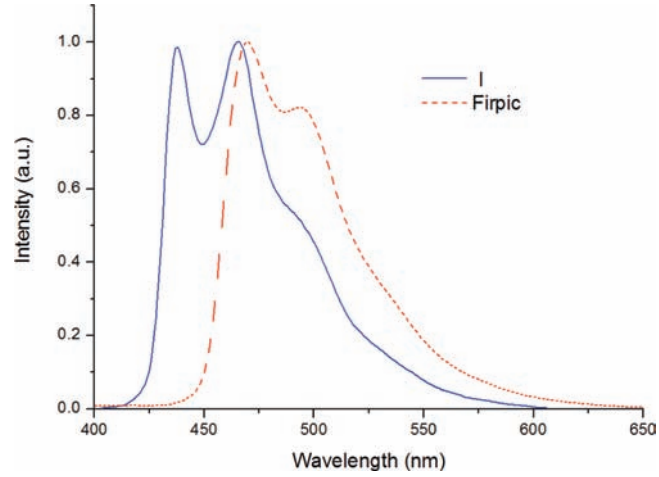

Figure 4. Emission spectra of **1** and FIrpic under the same conditions.

($\lambda_{max} > 350$ nm) are metal-to-ligand charge-transfer (MLCT) transitions. The next long tail absorption in the region of 420−450 nm can reasonably be assigned to a mixed state involving both spin−orbit coupling enhanced $^3\pi-\pi^*$ and ^{3}MLCT transitions.[3a] The blue-shifted ^{1}MLCT band (λ_{max} = ca. 360 nm, $\varepsilon = 8200\ M^{-1}\ cm^{-1}$) for complex **1** compared to that of FIrpic (λ_{max} = ca. 375 nm, $\varepsilon = 7500\ M^{-1}\ cm^{-1}$) was observed under the same experimental conditions. The intensities of ^{1}MLCT and ^{3}MLCT in **1** are stronger than those of the reference (FIrpic). This observation implies the presence of remarkable singlet−triplet coupling due to spin−orbit coupling in **1**. This result can be attributed to the introduction of the electron-withdrawing pyridine ring, as well as the fluorine substituents. Therefore, fluorine substituents and the replacement of phenyl with pyridine not only cause a spectral blue-shift for the $\pi-\pi^*$ and ^{1}MLCT absorptions but also increase the transition moment.

As shown in Figure 4, the emission spectrum of **1** is well structured, while the spectrum in FIrpic is less structured and broader than that of **1** (full-width at half-maximum (fwhm): 63nm for **1**, 56 nm for FIrpic). The emission maximum of **1** appears at 438 nm, and an additional intense peak appears at 463 nm. The intensity of each wavelength is almost the same, but the intensity at 463 nm is slightly higher than at 438 nm. In general, the emission band from MLCT states are broad and featureless, while the highly structured emission band mainly originates from the $^3\pi-\pi^*$ state.[19] Accordingly, the emission observed in **1** is attributable to the $^3\pi-\pi^*$ with contribution of the MLCT transition. The Commission Internationale de L'Eclairage (CIE) coordinates *x* and *y* for **1** were calculated to be 0.14 and 0.12, respectively, which is a high color purity and a purer blue than in FIrpic (CIE $x = 0.18$, $y = 0.34$).[18] The photoluminescence (PL) quantum yield in degassed CH_2Cl_2 solution at room temperature was determined to be 0.71(±10%) by using quinine sulfate in 0.1 N H_2SO_4 as the standard ($\Phi_{PL} = 0.54$). This value is slightly higher than that of FIrpic and comparable to that of Ir(dfppy)$_3$ (dfppy = 4,6-difluorophenylpyridine, $\Phi_{PL} = 0.77$). The rigidity of the molecular structure has an influence on the fluorescence quantum

(19) Hong, H.-W.; Chen, T.-M. *Mater. Chem. Phys.* **2007**, *101*, 170–176.

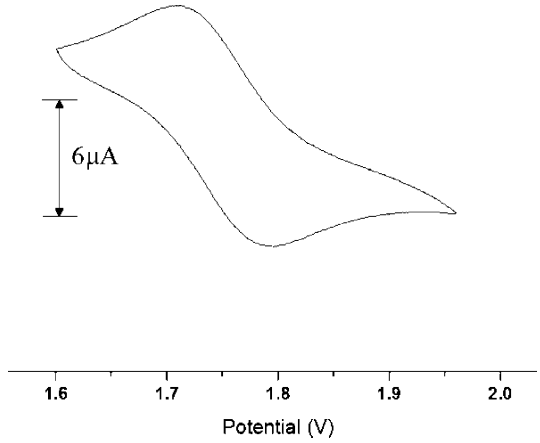

Figure 5. Cyclic voltammograms of **1** in 0.1 M *n*-Bu_4NPF_6 at a scan rate of 100 mV/s.

yields.[20] The replacement of C−H bonds with C−F bonds and the pyridine moiety introduced into the ligand bring about a lower vibrational frequency through the strong intermolecular interaction, leading to a reduced nonradiative decay rate and improved PL efficiency, as supported by the crystal structure.

To investigate the electronic effects caused by fluorine substituents on the bipyridine rings, cyclic voltammetry experiments including FIrpic were carried out (see Figure 5 and Supporting Information). Due to the limited range of CH_2Cl_2 and the limitations of our instrument to measure the reduction potentials in the range of −2.7∼−3.5 V, we obtained only reliable oxidation potentials. The reversible oxidation wave is observed for **1** at 1.78 V (E_{pa}). It is noteworthy that the complex shows higher oxidation potentials than that of FIrpic (E_{pa} = 1.45 V), indicating that a relative ease of oxidation does not exist. This can be ascribed to the greater electron-withdrawing ability of the fluorine atoms and pyridine ring. This observation implies that the HOMO energy level has been lowered by the introduction of the fluorine atoms into the 2′,4′-position of the 2,3′-bipyridine ligand. Furthermore, the replacement of the picolate ligand in FIrpic with difluorobipyridine resulted in an additional lowered HOMO level.

To understand the nature of the luminescence exhibited by **1**, DFT calculations were conducted employing the Gaussian-98 package. The initial geometric parameters in the calculations were employed from crystal structure data for geometry optimization. The experimental values of bond lengths, which were obtained from the X-ray structure, are comparable to the calculated values. The contour plots of the three lowest unoccupied (LUMO, LUMO + 1, and LUMO + 2) and the three highest occupied molecular orbitals (HOMO, HOMO − 1, and HOMO − 2) for **1** mainly involved in the transitions are presented in Figure 6. The calculated energy levels of the lowest singlet and triplet states are depicted in Table 3. As shown Figure 6, the HOMO of **1** involves the contribution of Ir d_{z^2} orbital (60%) with the contribution (ca. 35∼40%) from a π orbital localized on the fluorine-substituted pyridine ring. However, the LUMO is largely dominated by the π^* orbitals of the pyridine rings with small contributions of the π^* orbitals of the fluorine-substituted pyridine ring. To investigate the effect of the fluorine substituents, the comparison of energy levels of both $Ir(ppy)_3$ and **1** was conducted in Figure 7. For **1**, the energies of the HOMO and LUMO are lowered by about 1.60 and 1.04 eV, respectively, as compared to those of $Ir(ppy)_3$. The decrease of the HOMO level is a little deeper, indicating that the fluorine substituents and the replacement of pyridine have significant influence on the HOMO energy levels. Since the lowering of the HOMO in general induces a narrowing energy barrier between the dopant and the host or electron-transporting (ET) materials in OLEDs, this observation (HOMO lowered) makes complex **1** suitable for the easy transfer of electrons from the host or ET materials. The donation of d oritals of the Ir atom for **1** is significantly higher than in $Ir(ppy)_3$ or even FIrpic. The calculated electron populations of the three HOMOs for **1** are from 58% to 60%, while the d orbital populations of both $Ir(ppy)_3$ and FIrpic are below 50% based on the results of previous reports.[9,21] This implies that complex **1** shows strong spin−orbit mixing between the π and d orbitals of the Ir atom. It is noteworthy that significant contributions of the Ir metal (d orbital) in the LUMO level were not observed. The energy gap between the HOMO (−6.39 eV) and LUMO (−2.26 eV) is 4.13 eV. As shown in Table 3, complex **1** exhibits a larger energy gap relative to other Ir(III) derivatives (energy gap: 3.66 eV for $Ir(ppy)_3$, 3.75 eV for FIrpic, respectively).[22] The excitation energies for the low-lying singlet and triplet states of **1** were obtained from time-dependent DFT (TDDFT) calculations. Excitation energies for a singlet (S1) and a triplet (T1) state are 3.33 eV (372 nm) and 2.97 eV (417 nm), respectively. Experimentally, we observed that the ^{1}MLCT and ^{3}MLCT bands of **1** in the UV/vis spectrum were at 361 and 428 nm, respectively. Therefore, these results are in agreement with experimental values despite some deviations. The small deviation of the current theoretical approach from the experimental results is probably due to experimental difficulties in determining the absorption peak frequency.[22] According to these results, both calculated S1 and T1 excited states could be assigned as MLCT states based on the strong 5d component of the occupied orbitals and the mostly ligand π^*(py) virtual orbitals. These DFT calculations provide evidence that the luminescence observed in complex **1** originates from the Ir-perturbed ligand-centered transitions.

In summary, a new type of *fac*-Ir(III) complex containing fluorinated bipyridine as a ligand has been synthesized to investigation the effects of the substituents on the nature of its solid state, photoluminescence, and electrochemical behaviors. In addition, to understand the origin of the luminescence, DFT calculations were also conducted. The

(20) (a) Morrison, D. J.; Trefz, T. K.; Piers, W. E.; McDonald, R.; Parvez, M. *J. Org. Chem.* **2005**, *70*, 5309–5312. (b) Endo, A.; Suzuki, K.; Yoshihara, T.; Tobita, S.; Yahiro, M.; Adachi, C. *Chem. Phys. Lett.* **2008**, *460*, 155–157.

(21) Park, N. G.; Choi, G. C.; Lee, Y. H.; Kim, Y. S. *Curr. Appl. Phys.* **2006**, *6*, 620–626.

(22) Tung, Y.-L.; Chen, L.-S.; Chi, Y.; Chou, P.-T.; Cheng, Y.-M.; Li, E. Y.; Lee, G.-H.; Shu, C.-F.; Wu, F.-I.; Carty, A. J. *Adv. Funct. Mater.* **2006**, *16*, 1615–1626.

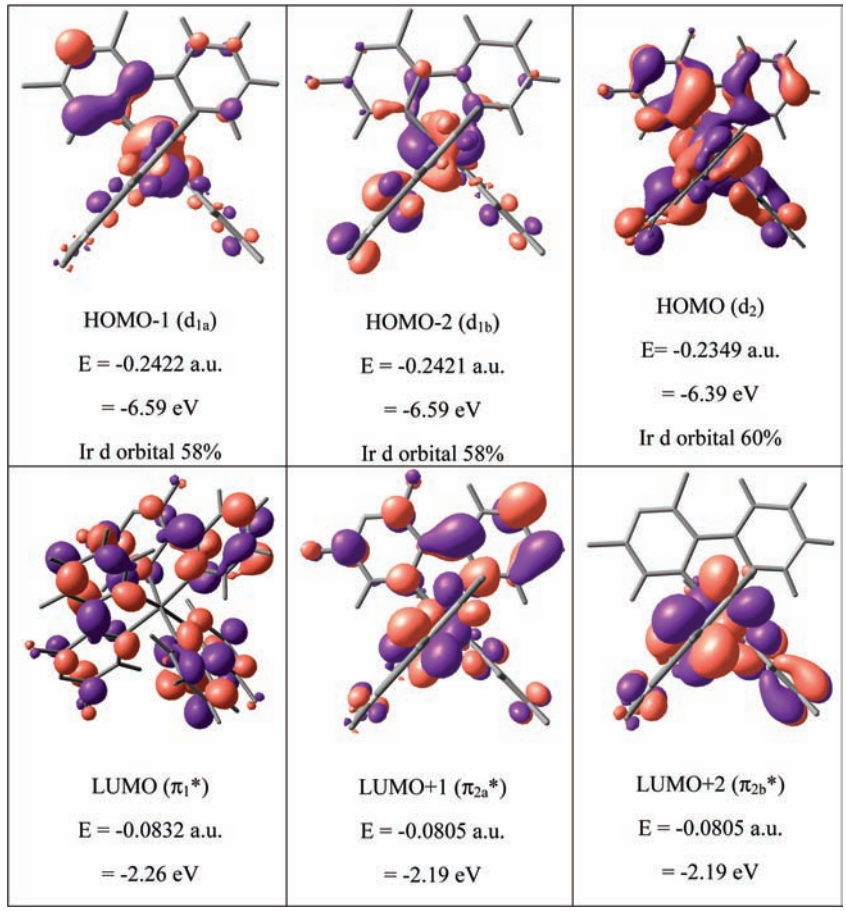

Figure 6. Diagrams showing the surfaces and energies of selected frontier orbitals for **1**.

Table 3. Calculated Energy Levels of the Low-Lying Singlet and Triplet States

spin state	(nm)	assignment (%)	*f*
S_1	372 (3.33 eV)	HOMO → LUMO (96%)	0.0043
	369 (3.36 eV)	HOMO → LUMO + 1 (95%)	0.0015
S_2	369 (3.36 eV)	HOMO → LUMO + 2 (95%)	0.0015
		HOMO-1 → LUMO (4%)	
S_3	347 (3.58 eV)	HOMO-1 → LUMO + 2 (45%)	0.0042
		HOMO-2 → LUMO (42%)	
		HOMO-5 → LUMO (5%)	
		HOMO-2 → LUMO + 1 (10%)	
	417 (2.97 eV)	HOMO → LUMO + 1 (12%)	
		HOMO-4 → LUMO + 1 (15%)	
		HOMO → LUMO (38%)	
		HOMO → LUMO (5%)	
		HOMO-3 → LUMO + 2 (7%)	
		HOMO-1 → LUMO + 2 (7%)	
T_1	417 (2.97 eV)	HOMO-4 → LUMO (10%)	
		HOMO → LUMO+2 (20%)	
		HOMO → LUMO+1 (25%)	
	417 (2.97 eV)	HOMO-3 → LUMO (9%)	
		HOMO-3 → LUMO+1 (4%)	
		HOMO-3 → LUMO+2 (7%)	
		HOMO → LUMO (9%)	
		HOMO → LUMO+1 (12%)	
		HOMO → LUMO (28%)	

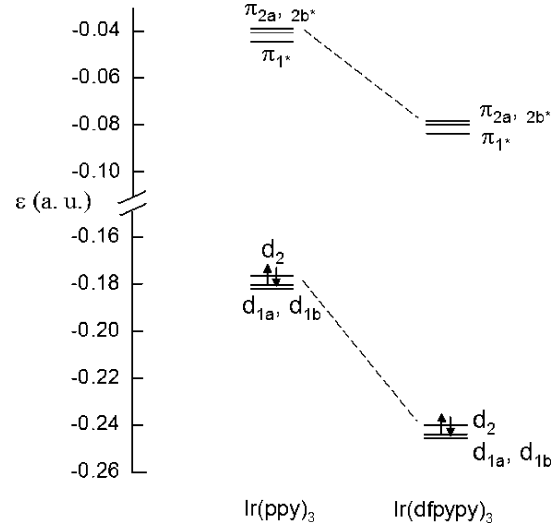

Figure 7. Schematic drawing of orbital energies of highest occupied and lowest unoccupied MOs of Ir(dfpypy)$_3$ from B3LYP calculations. The orbital energies of Ir(ppy)$_3$ were cited from ref 9 for the purpose of comparison. HOMO, HOMO − 1, and HOMO − 2 were denoted d_2, d_{1a}, and d_{1b}. LUMO, LUMO + 1, and LUMO + 2 were denoted π_{1*}, π_{2a}, and π_{2b*}. (1 au = 27.212 eV)

Ir(III) complex provided bright blue phosphorescence with high color purity ($x = 0.14$, $y = 0.12$), which is most likely caused by MLCT transitions. The replacement of the phenyl ring in ppy with pyridine and the introduction of fluorine substituents into the pyridine ring significantly increased the thermal stability and molecular rigidity due to the increased intermolecular interactions in the solid state. Based on DFT calculations, the substituents have significant effect on lowering the HOMO and LUMO energy levels, where the diminution of the HOMO energy is much larger than in the LUMO. It suggests that the complex **1** has disadvantages for hole injection. However, the lower LUMO level makes this complex suitable for the easy transfer of electrons from the electron-transporting layer. Therefore, further studies of

this complex may lead to a new class of emitting materials for phosphorescence OLEDs.

Acknowledgment. This study was supported by a 2007 Research Grant from Kangwon National University.

Supporting Information Available: X-ray crystallographic data, spectroscopic data (NMR, mass, etc.), and UV/vis and PL spectra. X-ray crystallographic files are available free of charge via the Internet at http://pubs.acs.org.

IC801643P